Hydroacoustically Aided Inertial Navigation for Joint Position and Attitude Estimation in Absence of Magnetic Field Measurements

Bård B. Stovner[1], Tor A. Johansen[2]

***Abstract*— When an underwater intervention vehicle is close to large metallic structures, e.g. subsea oil and gas facilities, magnetic disturbances might render magnetic field measurements biased or useless. This loss of information is critical for attitude estimation, and consequently, for the safety of the operation. In this paper, a three-stage filter for joint position and attitude estimation is developed, replacing the magnetic field measurements with hydroacoustic measurements. This solution assumes a hydroacoustic sensor set up with multiple transponders on the sea floor and 3 or more transceivers on the vehicle. The three-stage filters is shown to yield GES error dynamics of both the translational and rotational motion. The three-stage filter is shown in simulations to successfully estimate both the true position and attitude of the vehicle.**

I. Introduction

Inertial navigation integrates accelerometer and angular rate sensor (ARS) measurements to update position, velocity, and attitude estimates. When the inertial measurements are noisy and biased, the integration leads to a growing error in the estimates. In aided inertial navigation, other measurements are included to eliminate the drifting error in the inertial navigation. For the positioning, the aiding measurements are often range measurements. In underwater applications, these are usually provided by hydroacoustic systems such as long baseline (LBL), short baseline (SBL), ultrashort baseline (USBL) or inverted USBL (iUSBL) [1], [2], [3], [4]. In LBL, one transceiver on the vehicle aqcuires ranges from multiple transponders on the sea bed. SBL is similar, except the transponders are mounted to the underside of the surface vessel from which the underwater vehicle is usually deployed. In USBL, the underside of the surface vessel is equipped with a compact array of transceivers which measure the relative phase angles of a signal sent from a transponder mounted on the underwater vehicle. In iUSBL, this is reversed, placing the array of transceivers on the underwater vehicle and the transponder in a known location, e.g. on a surface vessel, the sea bed, or on an underwater structure. In this paper, the inverted SBL (iSBL) set up suggested by Stovner, Johansen, and Schjølberg [5] is assumed available, in which multiple transceivers are mounted to the underwater vehicle. Contrary to the iUSBL, the transceivers in the iSBL should be spaced out as much as possible, thus confining the baseline lengths to the size of the underwater vehicle and not to the size of the USBL apparatus in iUSBL. In addition to iSBL, it is assumed that there are two or more transponders in the vehicle's surroundings.

For attitude estimation, the growing error in inertial navigation is eliminated by reference vector measurements. These are vectors that are known or measured in both the body-fixed and the inertial frame, i.e. they only differ by the rotation between the two frames. Two reference vectors are sufficient to uniquely determine the vehicle's attitude. For applications on earth, it is common to use earth's gravitational and magnetic fields as reference vectors. They are known both in the inertial frame, given the approximate location on earth, and can be measured by an accelerometer and a magnetometer or compass in the body-fixed frame, respectively. When using an accelerometer to measure the gravity vector, it is sometimes assumed that the vehicle is weakly accelerated. This is done in Hamel and Mahony [6] and Mahony, Hamel, and Pflimlin [7]. By estimating the specific force, i.e. the sum of gravity and acceleration of the vehicle, in the inertial frame, this assumption can be lifted, as was done in Hua [8], Grip et al. [9], [10].

When an underwater intervention vehicle is near a subsea oil and gas facility, magnetic disturbances from the facility might render magnetic field measurements biased or useless. This is critical for the attitude estimation, as two non-parallel reference vectors are needed. In this paper, the magnetometer measurements are replaced by hydroacoustics, using iSBL with two or more transponders. A body-fixed three-stage filter is developed for estimation in this circumstance. It is conceptually similar to the three-stage filters in Stovner et al. [11], Johansen, Fossen, and Goodwin [12], both of which build on the theory of the exogenous Kalman filter (XKF) and the double Kalman filter (DKF) of Johansen and Fossen [13], [14]. Contrary to these works, which estimate the vehicle's position in the inertial frame, the body-fixed three-stage filter estimates the vehicle's position relative each transponder decomposed in the body-fixed frame. This was done in Stovner, Johansen, and Schjølberg [5] with one transponder when magnetic field measurements were available. This work is an extension of [5] to multiple transponders for estimation of both the translational and angular motion when magnetic field measurements are not used. When multiple transponders are available, the magnetic reference vector can be replaced by the baselines between the transponders. These are known in the inertial frame, and can be found by subtracting one of the body-fixed position states from an other. The same idea was presented in Batista, Silvestre, and Oliveira [15] except using only transponder baselines as reference vectors in the attitude estimation, and

[1]Bård B. Stovner is affiliated with the Centre of Autonomous Marine Operations and Systems (NTNU-AMOS), Department of Marine Technology, University of Science and Technology (NTNU), 7491 Trondheim, Norway.

[2]Tor A. Johansen is affiliated with NTNU-AMOS, Department of Engineering Cybernetics, NTNU, 7491 Trondheim, Norway.

not the gravitational field and accelerometer measurement vectors as is done here. Also, the estimation technique is different, as [15] relies on state augmentation to deal with non-linearities, while this work uses a three-stage filter that avoids augmentation. Both works, however, achieve globally exponentially stable (GES) estimates.

A. Contribution and Outline

In this paper, a novel GES three-stage filter is developed that achieves joint attitude and position estimation using an iSBL set up with two or more transponders in the vehicle's surroundings in the absence of magnetic field measurements.

In Section II, the dynamic model and measurement model are given. In Section III, the body-fixed three-stage filter is developed, before its stability is analyzed in Section IV. Simulation results and discussions follow in Section V and VI, respectively.

II. Models and Preliminaries

A. Notation

The vectors denoting the position, velocity, and angular rate of $\{c\}$ relative $\{b\}$ decomposed in frame $\{a\}$ are denoted p^a_{bc}, v^a_{bc}, and ω^a_{bc}, respectively. A rotation matrix expressing the rotation from the frame $\{a\}$ to $\{b\}$ is denoted R^a_b.

Using this notation, we define the translational state vector

$$x \triangleq \begin{bmatrix} p^b_{t_1 b} \\ \vdots \\ p^b_{t_N b} \\ v^b_{nb} \end{bmatrix} \tag{1}$$

where $p^b_{t_i b}$ is the position of the vehicle relative to the transponder $t_i, i \in [1, N]$ decomposed in the body-fixed frame $\{b\}$. v^b_{nb} is the body-fixed velocity of the vehicle relative the North-East-Down (NED) frame $\{n\}$.

We denote by $z = (R^n_b, b^b_{ars})$ the collection of variables R^n_b and b^b_{ars}, which are the rotation from the NED to the body-fixed frame and the ARS bias, respectively.

The matrices 0_n, $0_{n\times m}$ and I_n denote an $n \times n$ matrix of zeroes, an $n \times m$ matrix of zeroes and the identity matrix of dimension $n \times n$, respectively. The vector $l_n \in \mathbb{R}^n$ denotes a vector of ones.

B. Model

1) Measurements: On the vehicle, a transmitter s is placed, responsible for contacting the transponders. The transponders reply, and a hydrophone c_m, placed next to the transmitter, detects the time-of-arrival (TOA). From this, the distance plus noise $2\|p^b_{t_i b}+p^b_{bc_m}\|_2+\epsilon_{y,i}+\epsilon_{\partial,im}$ is measured. Now, the range measurement y_{im} is found

$$y_{im} = h_{im}(x) \triangleq \|p^b_{t_i b} + p^b_{bc_m}\|_2 + \frac{1}{2}\epsilon_{y,i} + \frac{1}{2}\epsilon_{\partial,im} \tag{2}$$

There are in total M hydrophones. The hydrophones $c_j, j = (1, ..., M)\backslash m$ also detect the TOA, but since the transmitter was placed next to hydrophone c_m, the distance measured by the TOA is $\|p^b_{t_i b}+p^b_{bc_m}\|_2+\|p^b_{t_i b}+p^b_{bc_j}\|_2+\epsilon_{y,i}+\epsilon_{\partial,ij}$. From this, y_{im} can be subtracted, yielding the range measurement model for y_{ij}

$$y_{ij} = h_{ij}(x) \triangleq \|p^b_{t_i b} + p^b_{bc_j}\|_2 + \frac{1}{2}\epsilon_{y,i} + \epsilon_{\partial,ij} - \frac{1}{2}\epsilon_{\partial,im} \tag{3}$$

Here, we assume that $\epsilon_{y,i} \sim \mathcal{N}(0, \sigma_y)^2$ is a white noise term common for the range measurements from transponder t_i to all hydrophones, while $\epsilon_{\partial,ij} \sim \mathcal{N}(0, \sigma_\partial)^2$ is unique for each hydrophone c_j. Since σ_y normally is much larger than σ_∂, it can be eliminated by considering the range difference measurements $\partial y_{ij}, j = (1, ..., M)\backslash m$

$$\begin{aligned} \partial y_{ij} &= \partial h_{ij}(x) \triangleq h_{ij}(x) - h_{im}(x) \\ &= \|p^b_{t_i b} + p^b_{bc_j}\|_2 - \|p^b_{t_i b} + p^b_{bc_m}\|_2 + \epsilon_{\partial,ij} - \epsilon_{\partial,im} \end{aligned} \tag{4}$$

Concatenating the above, we get

$$\begin{aligned} y &= \begin{bmatrix} y_1^\top & \cdots & y_N^\top \end{bmatrix}^\top \\ y_i &= \begin{bmatrix} y_{i1} & \cdots & y_{im} & \cdots y_{iM} \end{bmatrix}^\top \\ \partial y &= \begin{bmatrix} \partial y_1^\top & \cdots & \partial y_N^\top \end{bmatrix}^\top \\ \partial y_i &= \begin{bmatrix} \partial y_{i1} & \cdots & y_{im} & \cdots \partial y_{iM} \end{bmatrix}^\top \end{aligned}$$

and similarly for $h(x)$, $h_i(x)$, $\partial h(x)$, and $\partial h_i(x)$, respectively.

The ARS and accelerometer measurements are modelled as

$$\omega^b_{ars} = \omega^b_{nb} + b^b_{ars} + \epsilon_{ars} \tag{5}$$

$$f^b_{acc} = a^b_{nb} - R^{n\top}_b g^n + \epsilon_{acc} \tag{6}$$

respectively, where ω^b_{nb} and a^b_{nb} are the rotation and acceleration of the vehicle relative NED. The white noise terms ϵ_{ars} and ϵ_{acc} are assumed Gaussian with $\epsilon_{ars} \sim \mathcal{N}(0, \sigma^2_{ars})$ and $\epsilon_{acc} \sim \mathcal{N}(0, \sigma^2_{acc})$.

2) Dynamics: The dynamics of the rotational state is

$$\dot{R}^n_b = R^n_b S(\omega^b_{nb}) \tag{7a}$$

$$\dot{b}^b_{ars} = 0 \tag{7b}$$

where

$$S(\omega) = \begin{bmatrix} 0 & -\omega_3 & \omega_2 \\ \omega_3 & 0 & -\omega_1 \\ -\omega_2 & \omega_1 & 0 \end{bmatrix}$$

The dynamics of the translational motion state is

$$\dot{p}^b_{t_i b} = -S(\omega^b_{ars} - b^b_{ars} - \epsilon_{ars})p^b_{t_i b} + v^b_{nb} \tag{8a}$$

$$\dot{v}^b_{nb} = -S(\omega^b_{ars} - b^b_{ars} - \epsilon_{ars})v^b_{nb} + a^b_{nb} \tag{8b}$$

$$+ f^b_{acc} + R^{n\top}_b g^n - \epsilon_{acc} \tag{8c}$$

Concatenating (8) for N transponders yields

$$\dot{x} = A(t, z)x + B(z)u + G(x)\epsilon_x \tag{9}$$

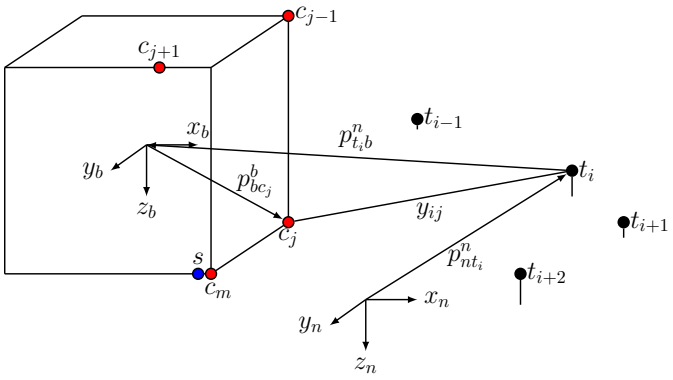

Fig. 1. The configuration of iSBL hydrophones (red), transmitter (blue), and LBL transponders (black)

where

$$A(t,z) = \begin{bmatrix} A_p(t,z) & L_N \\ 0_{3\times 3N} & -S(\omega^b_{ars} - b^b_{ars}) \end{bmatrix} \tag{10}$$

$$A_p(t,z) = \begin{bmatrix} -S(\omega^b_{ars} - b^b_{ars}) & \cdots & 0_{3N\times 3} \\ \vdots & \ddots & \vdots \\ 0_{3N\times 3} & \cdots & -S(\omega^b_{ars} - b^b_{ars}) \end{bmatrix}$$

$$A_p(t,z) \in \mathbb{R}^{3N\times 3N}, \quad L_N = \begin{bmatrix} I_3 \\ \vdots \\ I_3 \end{bmatrix} \in \mathbb{R}^{3N\times 3}$$

$$B(z) = \begin{bmatrix} 0_{3N\times 3} & 0_{3N\times 3} \\ I & R^\top(q^n_b) \end{bmatrix}, \; u(t) = \begin{bmatrix} f^b_{acc} \\ g^n \end{bmatrix} \tag{11}$$

$$G(x) = \begin{bmatrix} -S(p^b_{t_ib}) & 0_3 \\ \vdots & \vdots \\ -S(p^b_{t_ib}) & 0_3 \\ -S(v^b_{nb}) & -I_3 \end{bmatrix}, \epsilon_x = \begin{bmatrix} \epsilon_{ars} \\ \epsilon_{acc} \end{bmatrix} \tag{12}$$

III. Three-stage Body-fixed Filter

The structure of the three-stage filter can be seen in Figure 2. On the left-hand side, the estimation of the translational motion is done in three stages as in [12] and [14]. First, the range measurements go through an algebraic non-linear transformation (ANT), yielding a linear time-varying (LTV) measurement model from the non-linear in (2) and (3). This is used with the LTV dynamics to implement an LTV Kalman filter (KF) in the second stage. In the third stage, the non-linear measurement model in (2) and (4) is linearized about the estimate from the second stage. The linearized measurement model is used along with the linear dynamics to implement a linearized Kalman filter (KF). Through this cascade, the three-stage filter achieves the global stability of the LTV KF and the near-optimal performance associated with the linearized KF [13].

Stages two and three of the translational motion estimation described above rely on an attitude estimate to remove the gravity component from the accelerometer measurement (6). Since no magnetic field measurements are assumed in this paper, we are instead using the transponder baselines as reference vectors for attitude estimation. These are known

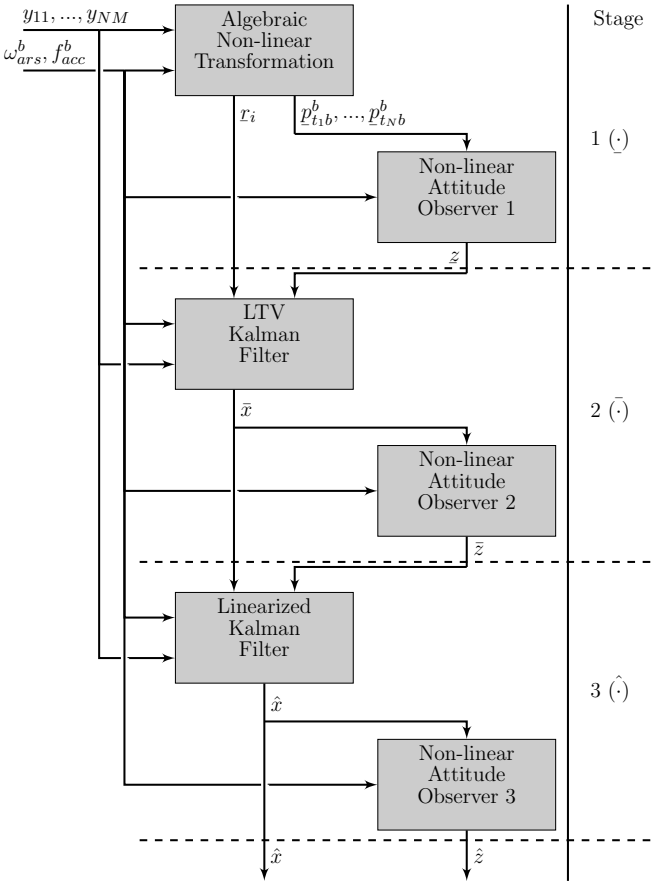

Fig. 2. In this figure, the three different stages of the body-fixed three-stage filter are depicted. The stage number and the associated notation can be seen on the right-hand side.

in NED and estimates of them in the body-fixed frame are found in each stage. Therefore, as can be seen on the right-hand side of Figure 2, the body-fixed three-stage filter implements three non-linear attitude observers (NLAO), i.e. one in each stage. While implementing three NLAOs instead of one may seem redundant, it is done in order to always use the best available transponder position estimates to estimate the attitude.

A. Stage 1

Stage 1 consists of an algebraic non-linear transformation and an NLAO. The former also calculates position estimates which the latter uses for attitude estimation.

In the derivation of the ANT, noise is neglected. By the algebraic manipulation, similar to that of Bancroft [16] and many others,

$$y^2_{ij} = \|p^b_{t_ib}\|^2 + 2{p^b_{bc_j}}^\top p^b_{t_ib} + \|p^b_{bc_j}\|^2 \tag{13}$$

we find the almost-linear model in $p^b_{t_ib}$

$$Y_i - l_M r_i = C_p p^b_{t_ib} \tag{14}$$

where

$$Y_i = \begin{bmatrix} y_{i1}^2 - \|p_{bc_1}^b\|^2 \\ \vdots \\ y_{iM}^2 - \|p_{bc_M}^b\|^2 \end{bmatrix}, C_p = \begin{bmatrix} 2p_{bc_1}^b{}^\top \\ \vdots \\ 2p_{bc_M}^b{}^\top \end{bmatrix} \tag{15}$$

$r_i = \|p_{t_ib}^b\|^2$, and $l_M \in \mathbb{R}^M$ is a vector of ones. Next, we find r_i explicitly in order to achieve a linear model from (14). Assuming that $M \geq 3$ and $\text{rank}(C_p) = 3$ we find

$$p_{t_ib}^b = -r_i c + w_i \tag{16}$$

where $c = C_p^\dagger l_M$, $w_i = C_p^\dagger Y_i$, and † denotes the Moore-Penrose pseudo-inverse. Now, inserting (16) into $r_i = \|p_{t_ib}^b\|_2^2$ yields

$$r_i^2\|c\|_2^2 - r_i \underbrace{(2c^\top w_i + 1)}_{h_i} + \|w_i\|_2^2 = 0$$

This is recognized as a scalar second-order equation with the two solutions

$$\underline{r}_i, \underline{\bar{r}}_i = \frac{h_i \pm \sqrt{h_i^2 - 4\|c\|_2^2\|w_i\|_2^2}}{2\|c\|_2^2}$$

Inserting $\underline{r}_i$ and $\underline{\bar{r}}_i$ into (16) will yield two positions, and the correct one can be found by auxilliary measurements or environmental knowledge. For example, one can rotate the two calculated positions to a local horizontal plane with roll and pitch angles directly calculated from the accelerometer measurements. The two resulting z-values can now be compared with depth measurements in order to determine the correct position, and thereby finding the correct value of r_i. Assuming we can solve this ambiguity, we select the correct solution and denote it $\underline{r}_i$. Using this in (14), we have successfully constructed the linear measurement equation

$$Y_i - l_M \underline{r}_i = C_p p_{t_ib}^b \tag{17}$$

Concatenating (17), we get the constructed linear measurement equation

$$Y = Cx \tag{18}$$

where

$$Y = \begin{bmatrix} Y_1 - l\underline{r}_1 \\ \vdots \\ Y_N - l\underline{r}_N \end{bmatrix}, \; C_{Np} = \begin{bmatrix} C_p & \cdots & 0_{M\times 3} \\ \vdots & \ddots & \vdots \\ 0_{M\times 3} & \cdots & C_p \end{bmatrix}$$

and $C = \begin{bmatrix} C_{Np} & 0_{NM\times 3} \end{bmatrix}$.

We also find an estimate of $p_{t_ib}^b$ to be used in the attitude observer

$$\underline{p}_{t_ib}^b = \underline{r}_i c + w \tag{19}$$

For attitude estimation in stage 1, we use the NLAO from Grip et al. [17]. The angular state estimate $\underline{z} = (R_{\underline{b}}^n, \underline{b}_{ars}^b)$ is found by

$$\dot{\underline{R}}_{\underline{b}}^n = \underline{R}_{\underline{b}}^n S(\omega_{ars}^b - \underline{b}_{ars}^b) + \underline{\sigma}\underline{K}_p J \tag{20a}$$

$$\dot{\underline{b}}_{ars}^b = -\text{Proj}(\underline{b}_{ars}^b, -\underline{k}_I \text{vex}(\mathbb{P}(\underline{R}_{\underline{b}}^{n\prime}\underline{K}_p J))) \tag{20b}$$

where

$$J = \sum_{i=1}^{N-1}\sum_{k=1}^{3}(\nu_{k,i}^n - \underline{R}_{\underline{b}}^n \nu_{k,i}^b)\nu_{k,i}^b{}^\top \tag{21a}$$

$$\nu_{1,i}^n = \frac{g^n}{\|g^n\|} \qquad \nu_{1,i}^b = \frac{f_{acc}^b}{\|f_{acc}^b\|} \tag{21b}$$

$$\nu_{2,i}^n = \frac{S(g^n)p_{t_it_N}^n}{\|S(g^n)p_{t_it_N}^n\|} \qquad \nu_{2,i}^b = \frac{S(f_{acc}^b)\underline{p}_{t_it_N}^b}{\|S(f_{acc}^b)\underline{p}_{t_it_N}^b\|} \tag{21c}$$

$$\nu_{3,i}^n = \frac{S^2(g^n)p_{t_it_N}^n}{\|S^2(g^n)p_{t_it_N}^n\|} \qquad \nu_{3,i}^b = \frac{S^2(f_{acc}^b)\underline{p}_{t_it_N}^b}{\|S^2(f_{acc}^b)\underline{p}_{t_it_N}^b\|} \tag{21d}$$

and $\underline{k}_I$, $\underline{K}_p$, and $\underline{\sigma}$ are tuning parameters. The function $\mathbb{P}(X) = \frac{1}{2}(X - X^\top)$ for a square matrix X, $\text{vex}(S(x)) = x$ for a vector $x \in \mathbb{R}^3$, and $\text{Proj}(\underline{b}_{ars}^b, \beta)$ is a projection function that ensures that the ARS bias estimate $\underline{b}_{ars}^b$ is kept inside a ball or radius M_b, in which the true ARS bias is assumed to lie. Notice that the use of g^n as a reference vector assumes a weakly accelerated vehicle, i.e. $f_{acc}^b \approx R^\top(q_b^n)g^n$. We have here arbitrarily chosen that the baseline from transponders $(1, ..., N-1)$ to transponder N are used as reference vectors. The NED and body-fixed baseline vectors are found by $p_{t_it_N}^n = p_{nt_N}^n - p_{nt_i}^n$ and $\underline{p}_{t_it_N}^b = \underline{p}_{t_ib}^b - \underline{p}_{t_Nb}^b$, respectively.

B. Stage 2

For the translational motion estimation in stage 2, we define the estimator

$$\dot{\bar{x}} \triangleq A(t, \underline{z})\bar{x} + B(\underline{z})u(t) + \bar{K}(t)(Y - C\bar{x}) \tag{22}$$

where $\bar{K}(t)$ is the time-varying Kalman gain matrix. The tuning matrix $\bar{R}$ is chosen as

$$\bar{Q} = \text{E}(\epsilon_x \epsilon_x^\top) = \text{diag}([\sigma_{ars}^2 l_3^\top, \sigma_{acc}^2 l_3^\top]) \tag{23}$$

and the elements of the measurement covariance matrix for the measurements from transponder i, $\bar{R}_i$, is given by

$$\text{Cov}(Y_{ik}, Y_{ij}) = \begin{cases} y_{ik}y_{ij}(\sigma_y^2 + \sigma_\partial^2), & k \neq j \\ y_{ik}y_{ij}(\sigma_y^2 + 5\sigma_\partial^2), & k = j \end{cases} \tag{24a}$$

$$\text{Cov}(Y_{ij}, Y_{im}) = y_{ij}y_{im}(\sigma_y^2 - \sigma_\partial^2) \tag{24b}$$

$$\text{Cov}(Y_{im}, Y_{im}) = y_{im}^2(\sigma_y^2 + \sigma_\partial^2) \tag{24c}$$

The full covariance matrix is given by $\bar{R} = \text{blkdiag}(\bar{R}_1, ..., \bar{R}_N)$, where blkdiag() creates a block-diagonal matrix from its input matrices. The G-matrix in the KF is $G(\bar{x})$.

For the angular motion estimation in stage 2, we implement the NLAO as in (20)–(21), except that $\underline{R}_{\underline{b}}^n$, $\underline{b}_{ars}^b$, $\underline{\sigma}$, $\underline{k}_I$, $\underline{K}_p$, and $\underline{p}_{t_it_N}^b$ are replaced by $\bar{R}_{\bar{b}}^n$, $\bar{b}_{ars}^{\bar{b}}$, $\bar{\sigma}$, $\bar{k}_I$, $\bar{K}_p$, and $\underline{\bar{p}}_{t_it_N}^{\bar{b}} = \underline{\bar{p}}_{t_ib}^{\bar{b}} - \underline{\bar{p}}_{t_Nb}^{\bar{b}}$, respectively.

C. Stage 3

In the third stage, the non-linear measurement model (2) and (4) is linearized about the estimate from stage 2. A KF is implemented, based on the linearized measurement model

and linear dynamics (9). The linearization of $h_{ij}(x)$ is found by the Taylor expansion

$$\partial h_{ij}(x) = \partial h_{ij}(\bar{x}) + H_{ij}(\bar{x})(x - \bar{x}) + \varphi(x, \bar{x}) \tag{25}$$

$$H_{ij}(\bar{x}) = \left.\frac{\mathrm{d}\partial h_{ij}(x)}{\mathrm{d}p^b_{t_ib}}\right|_{p^b_{t_ib}=\bar{p}^{\bar{b}}_{t_ib}} = \frac{(\bar{p}^{\bar{b}}_{t_ib} + p^b_{bc_j})^\top}{\|\bar{p}^{\bar{b}}_{t_ib} + p^b_{bc_j}\|_2} \tag{26}$$

where $\varphi(x, \bar{x})$ is the sum of higher order terms. Concatenating $H_{ij}(\bar{x})$ into a matrix yields

$$H(\bar{x}) = \begin{bmatrix} H_1 & \cdots & 0_{N\times 3} & 0_{N\times 3} \\ \vdots & \ddots & \vdots & \vdots \\ 0_{N\times 3} & \cdots & H_N & 0_{N\times 3} \end{bmatrix}, H_i = \begin{bmatrix} H_{i1} \\ \vdots \\ H_{iM-1} \end{bmatrix}$$

where the argument has been left out to simplify notation.

Now, we define the estimator

$$\begin{aligned}\dot{\hat{x}} =& A(t, \bar{z})\hat{x} + B(\bar{z})u(t) \\ &+ \hat{K}(t)(\partial y - \partial h(\bar{x}) - H(\bar{x})(\hat{x} - \bar{x}))\end{aligned} \tag{27}$$

where $\hat{K}(t)$ is the time-varying Kalman gain matrix. Since the dynamics of the LTV KF and the linearized KF of stage 2 and 3 are identical, we choose the process uncertainty matrix identically, i.e. $\hat{Q} = \bar{Q}$. The elements of the measurement uncertainty matrix for measurements $\partial y_{ij}, j = (1, ..., M)\backslash m$ and y_{im}, $\hat{R}_i$, is given by

$$\begin{aligned}\mathrm{Cov}(\partial y_{ij}, \partial y_{ik}) &= \mathrm{E}[(\epsilon_{\partial,ij} - \epsilon_{\partial,im})(\epsilon_{\partial,ik} - \epsilon_{\partial,im})] \\ &= \mathrm{E}(\epsilon_{y,ij}\epsilon_{y,ik}) + \mathrm{E}(\epsilon_{y,im}\epsilon_{y,im}) \\ &= \begin{cases} 2\sigma^2_\partial, k = j \\ \sigma^2_\partial, k \neq j \end{cases}\end{aligned} \tag{28a}$$

$$\begin{aligned}\mathrm{Cov}(\partial y_{ij}, y_{im}) &= \mathrm{E}[(\frac{1}{2}\epsilon_y + \frac{1}{2}\epsilon_{\partial,im})(\epsilon_{\partial,ij} - \epsilon_{\partial,im})] \\ &= -\frac{1}{2}\sigma^2_\partial\end{aligned} \tag{28b}$$

$$\mathrm{Cov}(y_{im}, y_{im}) = \mathrm{E}[(\frac{1}{2}\epsilon_y + \frac{1}{2}\epsilon_{\partial,im})^2] = \frac{1}{4}(\sigma^2_y + \sigma^2_\partial) \tag{28c}$$

and the full uncertainty matrix is given by $\hat{R} = \mathrm{blkdiag}(\hat{R}_1, ..., \hat{R}_N)$. The G-matrix used in this KF is $G(\bar{x})$.

For the angular motion estimation in stage 3, we implement the NLAO as in (20)–(21), except that $\underline{R}^n_{\bar{b}}$, $\underline{b}^b_{ars}$, $\underline{\sigma}$, $\underline{k}_I$, $\underline{K}_p$, and $\underline{p}^b_{t_it_N}$ are replaced by $\hat{R}^n_{\hat{b}}$, $\hat{b}^{\hat{b}}_{ars}$, $\hat{\sigma}$, $\hat{k}_I$, $\hat{K}_p$, and $\hat{p}^{\bar{b}}_{t_it_N} = \hat{p}^{\bar{b}}_{t_ib} - \hat{p}^{\bar{b}}_{t_Nb}$, respectively.

IV. Stability Analysis

The stability analysis of the body-fixed three-stage filter is conducted as follows: First, the stability of the NLAO states $\underline{z}$, $\bar{z}$, and $\hat{z}$ is collectively analyzed provided exact transponder baseline estimates $\underline{p}^b_{t_ib}$, $\bar{p}^b_{t_ib}$, and $\hat{p}^{\bar{b}}_{t_ib}$, respectively. Second, the translational motion estimator in each stage is analyzed. Lastly, the stability of the entire cascade is analyzed. This is a deterministic analysis, meaning we analyze the stability without noise. Before the analysis, we need to state two assumptions:

Assumption 1: There are at least $M \geq 3$ non-collinear transceivers on the vehicle.

Assumption 2: There are at least $N \geq 2$ transponders in the vehicle's surroundings, and the baseline between them is not parallel with the local gravitational field.

Proposition 1: Define $\tilde{\underline{z}} \triangleq (R^n_b - \underline{R}^n_{\underline{b}}, b^b_{ars} - \underline{b}^b_{ars})$, $\tilde{\bar{z}} \triangleq (R^n_b - \bar{R}^n_{\bar{b}}, b^b_{ars} - \bar{b}^b_{ars})$, and $\tilde{\hat{z}} \triangleq (R^n_b - \hat{R}^n_{\hat{b}}, b^b_{ars} - \hat{b}^b_{ars})$. Let $\dot{z} = (\dot{R}, \dot{b})$ and $z = 0$ only when $z = (R, b) = (0, 0)$.

1) Assuming $\underline{p}^b_{t_ib} = p^b_{t_ib}$, we have that the equilibrium point $\tilde{\underline{z}} = 0$ of the noise-free dynamics $\dot{\tilde{\underline{z}}}$ is GES under Assumption 2.
2) Assuming $\bar{p}^{\bar{b}}_{t_ib} = p^b_{t_ib}$, we have that the equilibrium point $\tilde{\bar{z}} = 0$ of the noise-free dynamics $\dot{\tilde{\bar{z}}}$ is GES under Assumption 2.
3) Assuming $\hat{p}^{\bar{b}}_{t_ib} = p^b_{t_ib}$, we have that the equilibrium point $\tilde{\hat{z}} = 0$ of the noise-free dynamics $\dot{\tilde{\hat{z}}}$ is GES under Assumption 2.

Proof: The proof for points 1–3 in Proposition 1 follows directly from Grip et al. [17]. ■

Proposition 2: Assume the rotation matrix and ARS bias estimates in stage 1 are exact, i.e. $R^n_{\bar{b}} = R^n_b$ and $\underline{b}^b_{ars} = b^b_{ars}$. Under Assumption 1, the equilibrium point $\tilde{\bar{x}} = 0$ of the second stage noise-free error dynamics $\dot{\tilde{\bar{x}}} = (A(t, \underline{z}) - \bar{K}(t)C)\tilde{\bar{x}}$ is GES.

Proof: For a general linear time-varying system with the process and measurments matrices $A(t)$ and $C(t)$, respectively, Kalman and Bucy [18] proves that the error dynamics of an LTV KF based on $A(t)$ and $C(t)$ is uniformly globally asymptotically stable (UGAS) (which is equivalent to GES for LTV systems) if and only if the pair $(A(t), C(t))$ is uniformly completely observable (UCO). The pair is UCO if and only if the observability co-distribution formed by $A(t)$ and $C(t)$ has full rank, Theorem 6.O12 of Chen [19]. The top $2NM$ rows of the observability co-distribution formed by $A(t, z)$ and C is

$$\mathrm{d}\bar{\mathcal{O}} = \begin{bmatrix} C \\ CA(t, \underline{z}) \end{bmatrix} = \begin{bmatrix} C_{Np} & 0_{NM\times 3} \\ C_{Np}A_p(t, \underline{z}) & N \cdot C_p \end{bmatrix}$$

From Theorem 4.2 of Meyer [20], we know that the block-triangular matrix $\mathrm{d}\bar{\mathcal{O}}$ has full rank if the matrices on the block diagonal have full rank. Since the block diagonal matrices only consists of C_p, we need that $M \geq 3$ and $\mathrm{rank}(C_p) = 3$, both of which follow from Assumption 1. When the partial observability co-distribution $\mathrm{d}\bar{\mathcal{O}}$ has full rank, then the full observability co-distribution has full rank as well. This concludes the proof. ■

Proposition 3: Assume that the KF tuning matrices $\hat{R}$, $\hat{Q}$, and $\hat{P}(0)$ are symmetric and positive definite. Further assume that the rotation matrix and ARS bias estimates in stage 2 are exact, i.e. $R^n_{\bar{b}} = R^n_b$ and $\bar{b}^{\bar{b}}_{ars} = b^b_{ars}$. Under assumptions 1 and 2, the equilibrium point $\tilde{\hat{x}} = 0$ of the third stage noise-free error dynamics $\dot{\tilde{\hat{x}}} = (A(t, \bar{z}) - \hat{K}(t)H(\bar{x}))\tilde{\hat{x}}$ is GES.

Proof: Then, Theorem 2.1 of Johansen and Fossen [13] states that provided with a GES linearization point $\bar{x}$, the equilibrium point $\tilde{\hat{x}} = 0$ of the dynamics of $\dot{\tilde{\hat{x}}} = (A(t, \bar{z}) - \hat{K}(t)H(\bar{x}))\tilde{\hat{x}}$ is GES if and only if the pair $(A(t, \bar{z}), H(\bar{x}))$ is UCO. By the same strategy as in Propo-

sition 2, it is straigh-forward to show that the observability co-distribution formed by $A(t, \bar{z})$ and $H(\bar{x})$ has full rank if the matrices $H_1(\bar{x}), ..., H_N(\bar{x})$ has full rank. This follows from Assumption 1, which concludes the proof. ■

Proposition 4: The equilibrium point $\tilde{z} = \tilde{\tilde{x}} = \tilde{\tilde{z}} = \hat{\tilde{x}} = \hat{\tilde{z}} = 0$ of the cascade of the respective noise-free error dynamics is GES.

Proof: Under Proposition 1, we know that the NLAOs in stage 1–3 are GES assuming they are provided with perfect baseline estimates. Under Proposition 2–3, we know that the translational motion estimation errors $\tilde{\tilde{x}}$ and $\hat{\tilde{x}}$ converge uniformally, globally, and exponentially to zero provided perfect attitude estimates. In the noise-free case, the ANT provides perfect baseline estimates to the NLAO in stage 1, meaning the NLAO in stage 1 is proven GES by Proposition 1. It is proven in Loria and Panteley [21] that a cascade of GES systems is GES. This can be used iteratively to prove that the cascade of estimators up until any of the estimators in stage 2 and 3 is GES, and thus, the whole cascade is GES. This concludes the proof. ■

V. Simulations

In the simulations, a vehicle with the dimensions $(L \times H \times W) = (1.2 \times 0.6 \times 0.6)m$ is assumed to be used. In four corners of the vehicle, a hydrophone is placed, i.e. $M = 4$ and

$$[p^b_{bc_1}, ..., p^b_{bc_M}] = \begin{bmatrix} 0.6 & 0.6 & 0.6 & -0.6 \\ 0.3 & 0.3 & -0.3 & 0.3 \\ 0.3 & -0.3 & 0.3 & 0.3 \end{bmatrix}$$

Furthermore, a transmitter is placed next to c_M, i.e. $m = M$.

The initial conditions are

$$p^n_{nb}(0) = \begin{bmatrix} 0 \\ 0 \\ 0 \end{bmatrix}, v^n_{nb}(0) = \begin{bmatrix} 0 \\ 0 \\ 0 \end{bmatrix} R^n_b(0) = I_3$$

the ARS bias is $b^b_{ars} = [0.012, -0.021, 0.014]^\top$, and the noise standard deviations are

$$\sigma_{acc} = 0.01 \frac{m}{s^2} \qquad \sigma_{ars} = 0.01 \frac{rad}{2} \qquad \sigma_{mag} = 0.01$$
$$\sigma_y = 1m \qquad \sigma_\partial = 0.01m$$

There are two transponders, i.e. $N = 2$, which are placed at $p^n_{nt_1} = [50, 50, 0]^\top$ and $p^n_{nt_2} = [-50, -50, 0]^\top$.

The estimate of the initial state of the vehicle is

$$\check{p}^n_{nb} = \begin{bmatrix} 10 & -10 & 5 \end{bmatrix}^\top, \check{v}^n_{nb} = \begin{bmatrix} 0 & 0 & 0 \end{bmatrix}^\top$$
$$\begin{bmatrix} \check{\phi} & \check{\theta} & \check{\psi} \end{bmatrix} = \begin{bmatrix} 5^\circ & 10^\circ & 20^\circ \end{bmatrix}$$
$$\check{b}^{\check{b}}_{ars}(0) = \begin{bmatrix} 0 & 0 & 0 \end{bmatrix}^\top$$

from which the estimates of all estimators are derived. The initial covariance matrices of the LTV KF and the linearized KF are $\bar{P}(0) = \hat{P}(0) = \text{blkdiag}(10I_3, 10I_3, 0.1I_3)$, respectively.

Even though the analysis was conducted in continuous-time, the KFs are implemented as discrete-time KFs.

The NLAO tuning parametres are chosen as $\underline{\sigma} = \bar{\sigma} = \hat{\sigma} = 1$, $\underline{K}_p = \text{diag}(1, 1, 8)$, $\bar{K}_p = \text{diag}(1, 1, 4)$, $\hat{K}_p = \text{diag}(1, 1, 10)$, $\underline{k}_I = .01 = \bar{k}_I = .01$, and $\hat{k}_I = 0.015$. In order to speed up convergence, the tuning parameters K_p and k_I are set to $10I_3$ and 0.1 in stages 1, 2, and 3 for the first 60, 120, and 180 seconds, respectively.

In the simulations, the vehicle stands still for the first 180 seconds to let the estimators to converge. Then, it descends and moves in a lawnmower pattern for 400 seconds, after which it stops. In the remainder of the 1000 seconds long simulation, the vehicle stands still. The results can be seen in Figure 3–6.

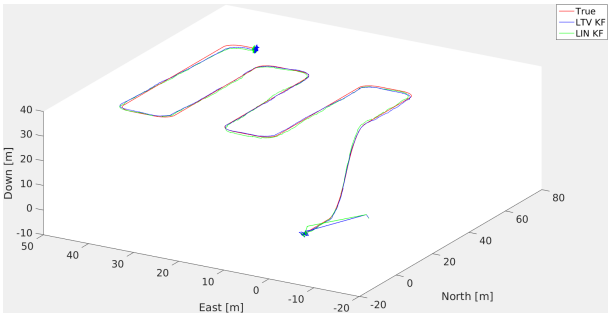

Fig. 3. The simulated trajectory of the vehicle.

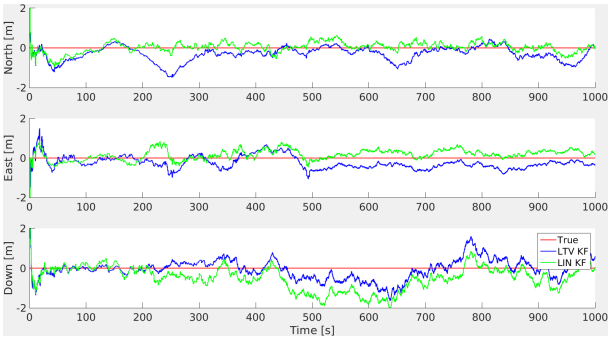

Fig. 4. This figure shows the north, east, and down position estimate errors from stage 2 and 3, found by transforming the position estimates to NED positions, i.e. to p^n_{nb}, and averaging them. The attitude estimate from the respective stages were used to rotate the body-fixed position estimates to the NED frame.

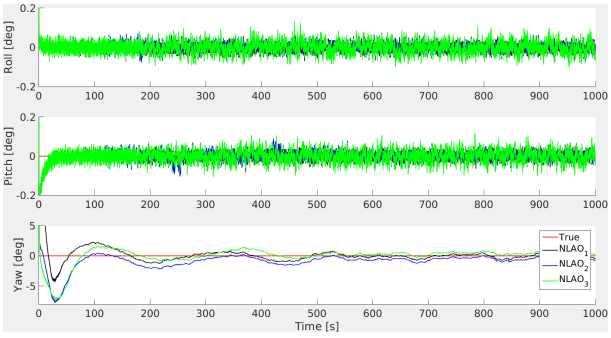

Fig. 5. Here, the attitude error in Euler angles are shown. They are found by extracting the Euler angles from $R^{\dot{b}}_{\dot{b}} = R^{n\top}_b R^n_{\dot{b}}$, where $(\dot{\cdot})$ is a placeholder for $(\underline{\cdot})$, $(\bar{\cdot})$, and $(\hat{\cdot})$.

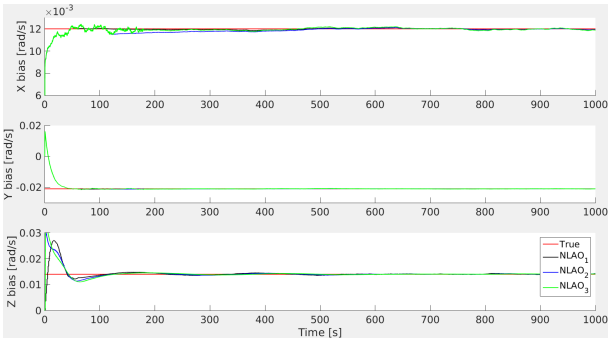

Fig. 6. Here, the ARS bias estimates of the three NLAOs are shown along with the true ARS bias.

VI. Discussion

In Figure 3, the trajectory that the vehicle follows is shown, along with the estimated positions. The position estimates from both the LTV KF and the linearized KF converge rapidly and track the true trajectory satisfyingly. This is confirmed in Figure 4 which clearly shows that both filters converge almost instantaneously. In Figure 4, we can also see that the linearized KF position estimate tracks the true value when the LTV KF position estimates deviates from it for some time. This is especially seen in the north and east position estimates.

In Figure 5, the roll, pitch, and yaw angle errors for the three NLAOs are shown. The roll and pitch angles are virtually identical for the three NLAOs, which is expected since all use the graviational field and accelerometer measurement reference vectors which are available at 100 Hz. The yaw angle, on the other hand, is only observed through the baseline vectors that are measured at 1 Hz. While the NLAOs in stage 2 and 3 have available baseline estimates from the LTV and linearized KFs at 100 Hz, new information that improve the baseline estimates are only available at 1 Hz. For this reason, we see a significantly slower convergence of the yaw estimate than of the roll and pitch estimates. Eventually, the three NLAOs successfully track the yaw angle. The same observation is made about the ARS bias estimates shown in Figure 6. While the three filters converge to the true value in all three directions, the yaw rate estimates converge significantly slower.

An observation about the body-fixed three-stage filter is that it is sensitive to the tuning of the NLAOs. This means that there probably is potential for tuning choices that yield better performance, and tuning them identically is probably not optimal. However, this is done here for simplicity and since the goal of this paper is not to show the optimal performance of the body-fixed three-stage filter, but rather to verify its usefulness.

VII. Conclusion

In this paper, a novel body-fixed three-stage filter for joint position and attitude estimation was developed. It relies on a hydroacoustic sensor network providing range measurements from 3 or more transceivers on the vehicle to two or more transponders in the vehicle's surroundings. Along with accelerometer and ARS measurements, this was shown to provide enough information for the estimation of both the body-fixed position of the vehicle relative to each transponder, the body-fixed velocity and the attitude of the vehicle, and the ARS bias. The stability of the filter was analyzed and it was shown to have GES error dynamics.

Acknowledgment

This work was partly supported by the Norwegian Research Council, grant no. 234108, through the Center of Autonomous Marine Operations and Systems (AMOS), grant no. 223254.

References

[1] K. Vickery, "Acoustic positioning systems. A practical overview of current systems," *Proceedings of the 1998 Workshop on Autonomous Underwater Vehicles (Cat. No.98CH36290)*, pp. 5–17, 1998.

[2] M. L. Neudorfer, "A Transponder Array Survey Method Using A Combined Short-Baseline/Long-Baseline Acoustic Position Reference System," in *Offshore Technology Conference*, Houston, 1978, pp. 113–118.

[3] J. C. Kinsey, R. Eustice, and L. L. Whitcomb, "A Survey of Underwater Vehicle Navigation: Recent Advances and New Challenges," in *7th Conference on Manoeuvring and Control of Marine Craft (MCMC'2006)*, 2006, pp. 1–12.

[4] O. Hegrenas, K. Gade, O. Hagen, and P. Hagen, "Underwater transponder positioning and navigation of autonomous underwater vehicles," *OCEANS 2009, MTS/IEEE Biloxi - Marine Technology for Our Future: Global and Local Challenges*, pp. 1–7, 2009.

[5] B. B. Stovner, T. A. Johansen, and I. Schjølberg, "Globally Exponentially Stable Aided Inertial Navigation with Hydroacoustic Measurements from One Transponder," in *Proc. of the American Contr. Conf., in-press*.

[6] T. Hamel and R. Mahony, "Attitude estimation on SO[3] based on direct inertial measurements," *Proceedings 2006 IEEE International Conference on Robotics and Automation, 2006*, pp. 2170–2175, 2006.

[7] R. Mahony, T. Hamel, and J. M. Pflimlin, "Nonlinear complementary filters on the special orthogonal group," *IEEE Transactions on Automatic Control*, vol. 53, no. 5, pp. 1203–1218, 2008.

[8] M. D. Hua, "Attitude estimation for accelerated vehicles using GPS/INS measurements," *Control Engineering Practice*, vol. 18, no. 7, pp. 723–732, 2010.

[9] H. F. Grip, T. I. Fossen, T. a. Johansen, and A. Saberi, "A nonlinear observer for integration of GNSS and IMU measurements with gyro bias estimation," *Proc. of the American Contr. Conf.*, pp. 4607–4612, 2012.

[10] H. F. Grip, T. I. Fossen, T. A. Johansen, and A. Saberi, "Attitude Estimation Using Biased Gyro and Vector Measurements With Time-Varying Reference Vectors," *IEEE Transactions on Automatic Control*, vol. 57, no. 5, pp. 1332–1338, 2012.

[11] B. B. Stovner, T. A. Johansen, T. I. Fossen, and I. Schjølberg, "Three-stage Filter for Position and Velocity Estimation from Long Baseline Measurements with Unknown Wave Speed," in *Proc. of the American Contr. Conf.*, 2016, pp. 4532–4538.

[12] T. A. Johansen, T. I. Fossen, and G. C. Goodwin, "Three-stage filter for position estimation using pseudo-range measurements," *IEEE Transactions on Aerospace and Electronic Systems*, 2016.

[13] T. A. Johansen and T. I. Fossen, "The eXogenous Kalman Filter (XKF)," *International Journal of Control*, 2016.

[14] ——, "Nonlinear Filtering with eXogenous Kalman Filter and Double Kalman Filter," in *Proceedings of European Control Conference*, 2016.

[15] P. Batista, C. Silvestre, and P. Oliveira, "GES integrated LBL/USBL navigation system for underwater vehicles," *Proceedings of the IEEE Conference on Decision and Control*, pp. 6609–6614, 2012.

[16] S. Bancroft, "An Algebraic Solution of the GPS Equations," *IEEE Transactions on Aerospace and Electronic Systems*, vol. AES-21, no. 1, pp. 56–59, 1985.

[17] H. F. Grip, T. I. Fossen, T. A. Johansen, and A. Saberi, "Globally exponentially stable attitude and gyro bias estimation with application to GNSS/INS integration," *Automatica*, vol. 51, no. June, pp. 158–166, 2015.

[18] R. E. Kalman and R. S. Bucy, "New results in linear filtering and prediction theory," *Journal of Basic Engineering*, vol. 83, no. 1, pp. 95–108, 1961.

[19] C.-T. Chen, *Linear System Theory and Design*, 3rd ed. Oxford University Press, Inc., 1998.

[20] C. D. MEYER, "Generalized Inverses and Ranks of Block Matrices," *SIAM Review*, vol. 25, no. 4, pp. 597–602, 1973.

[21] A. Loria and E. Panteley, "Cascaded nonlinear time-varying systems : analysis and design," in *Advanced Topics in Control Systems Theory*. Springer, 2005, ch. 2, pp. 23–64.